Brown Fat Paucity Due to Impaired BMP Signaling Induces Compensatory Browning of White Fat

Tim J. Schulz[1,6], **Ping Huang**[2], **Tian Lian Huang**[1], **Ruidan Xue**[1,3], **Lindsay E. McDougall**[1], **Kristy L. Townsend**[1], **Aaron M. Cypess**[1], **Yuji Mishina**[3], **Emanuela Gussoni**[2], and **Yu-Hua Tseng**[1,5,*]

[1]Section on Integrative Physiology and Metabolism, Joslin Diabetes Center, Harvard Medical School, Boston, MA, USA

[2]Program in Genomics and Division of Genetics, Children's Hospital, Harvard Medical School, Boston, MA, USA

[3]Division of Endocrinology and Metabolism, Huashan Hospital, Shanghai Medical College, Fudan University, Shanghai 200032, PR China

[4]Department of Biologic and Materials Sciences, School of Dentistry, University of Michigan, Ann Arbor, MI, USA

[5]Harvard Stem Cell Institute, Harvard University, Cambridge, MA, USA

Summary

Maintenance of body temperature is essential for survival of homeotherms. Brown adipose tissue (BAT) is a specialized fat tissue that is dedicated to thermoregulation[1]. Due to its remarkable capacity to dissipate stored energy and its demonstrated presence in adult humans[2-5], BAT holds great promise for the treatment of obesity and metabolic syndrome[1]. Rodent data suggest the existence of two types of brown fat cells: the constitutive BAT (cBAT), which is of embryonic origin and anatomically located in the interscapular region of mice, and the recruitable BAT (rBAT) that resides within white adipose tissue (WAT)[6] and skeletal muscle[7], that has alternatively been called beige[8], brite[9], or inducible BAT[10]. Bone morphogenetic proteins (BMPs) regulate the formation and thermogenic activity of BAT[10-12]. We here provide evidence for a systemically active regulatory mechanism that serves to control whole body BAT-activity for thermoregulation and energy homeostasis. Genetic ablation of type 1A BMP-receptor (*Bmpr1A*) in brown adipogenic progenitor cells leads to a severe paucity of cBAT. This in turn increases sympathetic input to WAT, thereby promoting the formation of rBAT within white fat depots.

*Corresponding author: Yu-Hua Tseng, Ph.D., Joslin Diabetes Center, One Joslin Place, Boston, MA 02215, Phone: 617-309-1967, Fax: 617-309-2650, Yu-Hua.Tseng@joslin.harvard.edu.
[6]Current address: Department of Adipocyte Development, German Institute of Human Nutrition, Potsdam-Rehbrücke, Germany

Author Manuscript

This previously unknown compensatory mechanism, aimed at restoring total brown fat-mediated thermogenic capacity in the body, is sufficient to maintain normal temperature homeostasis and resistance to diet-induced obesity. These data suggest an important physiological cross-talk between the constitutive and recruitable brown fat cells. This sophisticated regulatory mechanism of body temperature may participate in the control of energy balance and metabolic disease.

It has recently become clear that cBAT shares a common developmental ancestry with skeletal muscle[13,14], whereas rBAT, localized within white fat or skeletal muscle, derives from a non-myogenic lineage[10,13]. Lineage-tracing experiments have also revealed that cBAT arises from progenitors located in the embryonic dermomyotome[15] that express myogenic markers Pax7 and Myf5[13,16]. We thus generated a mouse model lacking BMPR1A in all cells descending from the Myf5^{pos} lineage (Myf5-BMPR1A-KO). No apparent changes in morphology, proliferation, or apoptosis were observed during early embryonic stages (Supplementary Fig. 1 and 2). Histological evidence of reduced cBAT-formation in Myf5-BMPR1A-KO mice was first observed at embryonic day 16.5 (E16.5) and persisted until after birth (P1, Fig. 1a-c). cBAT arises from highly proliferative fibroblasts during late gestational stages[17]. At E16.5, developing cBAT stains strongly for the proliferation marker Ki67, which was markedly decreased in Myf5-BMPR1A-KO embryos (Fig. 1d, Supplementary Fig. 2b and 2d). Apoptosis-levels were found unchanged throughout embryogenesis Supplementary Fig. 2c), suggesting that reduced proliferation occurring prior to or around E16.5 is responsible for defective formation of cBAT in KO animals.

Myf5-BMPR1A-KO mice were born runted and stayed smaller throughout life (Fig. 1e and 1f). Importantly, the reduction of cBAT mass remained highly significant in adult mice (Fig. 1g and 1h). Despite this, gene expression pattern of the residual cBAT appeared normal, apart from a moderate reduction of *Bmpr1A* gene expression (Supplementary Fig.3). The sizes of interscapular WAT (iWAT) and retroperitoneal WAT (rWAT), two white fat depots that contain subpopulations of cells from the Myf5^{pos} lineage[18], were also reduced in the KO-mice (Supplementary Fig. 4a). Gene expression in iWAT showed a trend towards reduced expression of BAT-genes, but no changes in general white adipogenic genes (Supplementary Fig. 4b). Subcutaneous WAT (sWAT) and epididymal WAT (eWAT), both mostly originating from a Myf5^{neg} lineage[18], were not decreased in size and expressed normal levels of all type-I BMP receptors (Fig. 1g-h, Supplementary Fig. 3a-c). Expression of *Bmpr1A* in skeletal muscle, on the other hand, was reduced by >95% (Supplementary Fig. 3a). Upon normalization to body weight, we found limb skeletal muscle size unchanged, while the function of myogenic progenitors was altered (Huang and Gussoni, unpublished data). Thus, loss of BMP-signaling in Myf5-expressing cells specifically targets the formation of cBAT. During embryogenesis, MyoD[pos] progenitors emerge after the Myf5^{pos} progenitors[19]. MyoD-CRE driven *Bmpr1A*-KO mice showed completely normal development of cBAT and WAT depots (Supplementary Fig. 5), suggesting that the developmental divergence between myogenic and brown adipogenic progenitors takes place prior to emergence of MyoD[pos] progenitors, or that BMPR1A is not required for cBAT-formation during this particular developmental stage.

A very similar phenotype was observed in a second mouse model with conditional deletion of *Bmpr1A* in all types of adipocytes (aP2-BMPR1A-KO). Loss of *Bmpr1A* led to a specific paucity of cBAT as well as WAT-resident rBAT (Supplementary Fig. 6). Since the aP2-CRE driver is active at later adipogenic stages compared to Myf5-CRE, we conclude that signaling through BMPR1A is essential also for later stages of brown adipogenesis.

Next, we isolated progenitors from either Myf5^{neg} sWAT or Myf5^{pos} cBAT to test their cell-autonomous ability to produce brown adipocytes[10]. Cells derived from sWAT differentiated normally (Supplementary Fig. 7). In contrast, the frequency and ability of cBAT-derived Myf5^{pos}/Sca1^{pos}/CD31^{neg} progenitors to differentiate into mature brown adipocytes was significantly reduced (Fig. 2a and 2b). We therefore generated brown pre-adipocytes from cBAT completely lacking BMPR1A (Supplementary Fig. 8a and 8b). Loss of *Bmpr1A* resulted in a marked inhibition of differentiation (Fig. 2c) and ability to respond to BMP7-induced phosphorylation of downstream targets of BMP-signaling, Smad and p38-mitogen activated protein kinase (p38MAPK)[20] (Fig. 2d). This led to a concomitant decrease of the expression of key adipogenic transcription factors *Zfp423*[21], *Cebpα*, and *Pparγ*[22] in undifferentiated pre-adipocytes (Fig. 2e). Following adipogenic differentiation, BMPR1A-KO cells displayed severely reduced expression of BAT-markers *Ucp1*, *Prdm16*[13], and *Pparγ* (Fig. 2f), even in the presence of BMP7. Aside from BMPR1A, BMPR1B and Activin A receptor, type 1 (ACVR1) are the other two major type 1 BMP-receptors[20]. While cBAT developed normally in whole body BMPR1B-KO-mice (Supplementary Fig. 9a and 9b), deletion of *Acvr1* in the Myf5^{pos} lineage resulted in a severe reduction of cBAT mass (Supplementary Fig. 9c and 9d), indicating that both ACVR1 and BMPR1A are essential for development of cBAT. Accordingly, pre-adipocytes lacking *Acvr1* displayed a somewhat milder phenotype compared to BMPR1A-deficient cells, while in double knock-out cells, brown adipogenesis was completely abolished (Supplementary Fig. 8c-g).

Since BAT plays a key role in thermoregulation, one would anticipate that the Myf5-BMPR1A-KO mice would display reduced body temperature as a consequence of impairment in cBAT-development. Indeed, newborn Myf5-BMPR1A-KO mice, with their unfavorable surface-to-volume ratio, showed a significant reduction in body temperature (Fig. 3a and 3b). This reduction in body temperature was surprisingly no longer present in adult Myf5-BMPR1A-KO (Fig. 3c, 22°C), suggesting a compensatory mechanism aimed at restoring thermogenic capacity. Non-shivering thermogenesis is a critical response to prolonged cold exposure in order to maintain body temperature[23]. When exposed to acute and chronic cold challenges, control mice were able to quickly resume normal body temperature after 48 h of cold, suggesting rapid activation of non-shivering thermogenesis via cBAT and possibly other short-term measures such as muscle shivering, which are less pronounced in newborn mice. By contrast, Myf5-BMPR1A-KO mice displayed a reduction in body temperature after 2 and 48 h of cold exposure, presumably due to the paucity of cBAT (Fig. 3c, 5°C-2h and -48h), as we did not observe any abnormal behavior, such as increased shivering, under cold exposure. Despite this, body temperature in Myf5-BMPR1A-KO mice returned to normal after prolonged cold exposure (i.e. 11 days), strongly suggesting an adaptive recruitment of rBAT to cope with lower ambient temperatures (Fig. 3c, 5°C-11d). Accordingly, KO-animals displayed a marked increase of UCP1-protein

expression in sWAT (Fig. 3d, Supplementary Fig. 10). This browning-effect could be further enhanced in sWAT, and induced in eWAT, by administration of the β3-adrenergic receptor agonist CL316,243, as signified by significantly increased expression of BAT-markers *Ucp1* and *Cidea* in Myf5-BMPR1A-KO mice (Fig. 3e-h), as well as increased emergence of multilocular UCP1^{pos} adipocytes in WAT (Fig. 3i and 3j).

Recruitable BAT is sensitive to inductive factors, such as BMP7[10,11], BMP8b[12], fibroblast growth factor (FGF)21[24], and the myokine irisin[25], among others. However, gene expression analysis revealed no changes in any of these (Supplementary Fig. 11), suggesting that the compensatory browning is not mediated by these factors. Since thermogenesis is rigorously controlled by the sympathetic nervous system (SNS)[26,27], we quantified sympathetic input to white fat in Myf5-BMPR1A-KO mice. Staining for tyrosine hydroxylase was significantly increased in sWAT of KO-mice (Fig 3k and 3l). Moreover, circulating levels of norepinephrine (NE) were also significantly elevated in KO-mice, suggesting that increased sympathetic input may contribute to the browning of WAT in Myf5-BMPR1A-KO mice (Fig. 3m). Additionally, cold-exposed Myf5-BMPR1A-KO mice displayed normal NE-induced thermogenic capacity (Fig. 3n, Supplementary Fig. 12), and thus possess a sufficient ability to compensate for loss of cBAT. These findings suggest that both types of brown fat may possess similar capacities for thermoregulation if maximally stimulated. Whereas cBAT is essential during acute cold challenges, compensatory rBAT in the KO-mice with severe paucity of cBAT plays a critical role in maintaining normal body temperature, especially during long-term cold exposure. In accordance with these findings, Myf5-BMPR1A-KO animals were resistant to diet-induced obesity, even under obesity-promoting thermoneutrality conditions, where mice no longer require thermogenesis to maintain body temperature[28] (Supplementary Fig. 13).

To determine whether the effect of compensatory browning is also present in other models of cBAT-atrophy and independent of genetic intervention that could also affect skeletal muscle, we surgically interrupted innervation of cBAT in wild-type mice. Denervation of cBAT resulted in a significant decrease of cBAT size and a 68% reduction of *Ucp1* expression in cBAT (p=0.0029; Fig. 4a and 4b). As in Myf5-BMPR1A-KO mice, atrophy of cBAT resulted in increased recruitment of brown adipocytes in WAT (Fig. 4c-e), thus reinforcing the notion of a systemic mechanism that regulates total BAT-mediated thermogenic capacity.

It has been documented before that surgical removal of cBAT causes an activation of the remaining depots of cBAT[29]. Here we utilize both genetic and surgically-generated models of cBAT paucity to demonstrate the existence of a physiological mechanism to ensure thermoregulation by compensatory browning of WAT. This type of BAT may be more closely related to that found in adult humans[8]. The system inducing formation of rBAT appears to involve cBAT-brain and brain-WAT communication that is mediated, at least in part, by the SNS. Interestingly, obesity-resistance in mice appears to be mostly related to browning of white fat, rather than adaptive thermogenesis of cBAT[30], altogether suggesting that rBAT is a key contributor to metabolic health. The findings presented here suggest that any therapeutic approach involving rBAT must take into account the tight regulation of total BAT-mediated thermogenic capacity and systemic energy metabolism at both peripheral and

possibly also central levels. Targeting these mechanisms, for instance by modifying BMP-signaling to regulate BAT mass and activity, could constitute a compelling approach to develop obesity therapies.

Full Methods

Animals

All animal procedures were approved by the Institutional Animal Use and Care Committee at Joslin Diabetes Center. Transgenic mice carrying floxed alleles for *Alk2/Acvr1*[31], or *Alk3/Bmpr1A*[32] were used to generate conditional gene deletion mouse models by intercrossing with either Myf5-[33] or aP2/FABP2-driven[34] CRE-expression as indicated. For studies involving *Alk6/Bmpr1B*-deletion, animals with whole body gene deletion of this receptor were used[35]. Myf5-CRE expressing animals were also crossed to Rosa26-YFP reporter mice (The Jackson Laboratory, Bar Harbor, ME) in addition to the *Bmpr1A*-flox alleles for Myf5-lineage-tracing and GFP-labeling of *Bmpr1A*-deficient cells as described before[10]. For genotyping, DNA was isolated from tail tip biopsies by boiling in 0.5 ml 50 mM NaOH for 15 min, followed by neutralization by addition of 50 μl 1M Tris-base (pH 6.8) and thorough vortexing. PCR-genotyping was performed using primers as listed in Supplementary Table S1. Expected band sizes for *Bmpr1A* during gel analysis were 180 bp for the wild type allele and 230 bp for the floxed allele. For recombination analysis of *Bmpr1A*-mRNA, expected band sizes were: 396 and 233 bp for the intact and recombined alleles, respectively, and 178 bp for the control PCR of exons 6 to 7. For Alk2-genotyping, the PCR product was subsequently digested using the restriction enzyme Bgl-I (New England Biolabs, Ipswich, MA) at 37°C overnight, yielding a band at 250 bp for wild type mice, and a double band at 90 bp and 160 bp for floxed alleles (all three bands in heterozygotes). Expected band sizes for *Bmpr1B* were 350 bp for the wild type, and 300 bp for the null allele. Expected band sizes for the Rosa26-YFP reporter mice were 600 bp for the wild type allele and 320 bp for the mutant allele. For Myf5-CRE genotyping, bands at 600 and 400 bp for wild type and mutant alleles, respectively, were expected. For a general CRE-PCR, a single band at approximately 350 bp indicated presence of CRE-cDNA in the genome. For loading control, IRS-1 primers were added for co-amplification in the same reaction (band at approximately 500 bp) to ensure proper loading with template DNA. To stimulate the browning of white adipose depots, mice were treated with daily i.p. injections of 1 mg/kg bodyweight CL316,243 (Sigma-Aldrich, St. Louis, MO) dissolved in PBS (also used for control injections) for up to ten days. For experiments involving high fat diet feeding, 4- to 6-week-old animals were placed on a diet containing 45 or 60 kcal% fat (Research Diets, New Brunswick, NJ). For cold exposure and thermoneutral conditions, animals were housed at 5°C or 30°C, respectively, for the indicated times in a controlled environmental chamber (Caron Products & Services Inc., Marietta, OH) with free access to food and water. Body core temperature was determined by rectal probe measurements.

Haematoxylin & Eosin staining

Sections were prepared, processed, and stained as described[11].

Immunofluorescence

Sections were deparaffinized and prepared as described before[11]. Primary antibodies were incubated overnight at 4°C: Ki67 (1:200, rabbit polyclonal; Abcam, Cambridge, MA); UCP1 (1:50, rabbit polyclonal; AnaSpec, Fremont, CA), Tyrosine hydroxylase (1:50, rabbit polyclonal, Millipore, Billerica, MA), GFP (1:200, goat polyclonal; Novus USA, Littleton, CO). After primary antibody incubation, the sections were washed and incubated with appropriate secondary antibody (AlexaFlour-488 (green) or -594 (red); Invitrogen, Carlsbad, CA) at a 1:200 dilution for 10 min in the dark. After secondary antibody incubation, sections were washed with distilled water for DAPI-staining (0.1 μg/ml in water for 5-10 minutes in the dark), and mounted. Sections were kept in the dark after mounting and analyzed by confocal microscopy on a Zeiss LSM-410 Invert Laser Scan Microscope (Carl Zeiss MicroImaging, Thornwood, NY), or using a florescence microscope (Olympus BX60F-3; Olympus Corporation, Center Valley, PA). Quantification of tyrosine hydroxylase was performed by using the ImageJ software (ImageJ, NIH, Bethesda, MD). Identical conditions and settings were used for picture acquisition and analysis. A threshold was set for each image to eliminate background and to create a binary mode image. A minimum particle size of 20 pixels was used as exclusion criteria to eliminate unspecific background and for quantification of areas that stained positive for tyrosine hydroxylase. For quantification of Ki67-staining, Ki67^{pos} nuclei were counted in areas identified as BAT by microscopic inspection of morphology and comparison to published sources[36], and normalized to the total number of DAPI[pos] nuclei in the same area. For each section and animal, images from three representative areas were analyzed.

TUNEL staining

For detection of DNA fragmentation, sections were deparaffinized and blocked for autofluorescence as described[10]. Sections were blocked in 1% BSA/ 0.5%-1% TX-100 in PBS for 1 h followed by washes in PBS. Terminal strand labeling was performed for 1.5 h at 37° C in TdT-buffer (30 mM Tris-HCL, 140 mM Na-Cacodylate, 1 mM Cobalt(II) chloride, pH 7.2) in the presence of dATP, biotinylated dUTP, and terminal deoxynucleotidyl transferase (all from Roche Applied Science, Indianapolis, IN). The reaction was stopped by immersion in $2\times$ SSC buffer and subsequent incubation with Cy3-labeled streptavidin (1:200; Jackson ImmunoResearch Laboratories, West Grove, PA) for 1 h in the dark. Sections were then stained with DAPI, mounted, and analyzed as described above.

RNA and protein quantification

RNA extraction, cDNA synthesis, and quantitative real-time PCR (qPCR) were performed as described before[11]. For qPCR analysis, ct-values <30 were used for gene expression analysis. Protein detection by western blotting was performed as described before[11]. Primary antibodies were incubated overnight at 4°C: phospho-Smad-1/5/8 (1:1000, rabbit polyclonal), Smad1 (1:1000, rabbit polyclonal), phospho-p38 MAPK (1:1000, rabbit polyclonal), p38-MAPK (1:1000, rabbit polyclonal) (all from Cell Signaling Technologies, Danvers, MA), UCP1 (1:500, goat polyclonal; Santa Cruz Biotechnology Inc., Santa Cruz, CA) and β-Tubulin (1:8000, mouse polyclonal; Sigma-Aldrich). HRP-coupled secondary

antibodies (Cell Signaling Technologies) were used at 1:2000 dilutions at room temperature for 2 h followed by detection using ECL-system.

Cell Sorting

Sca1[pos] adipocyte progenitor cells were isolated from constitutive brown adipose tissue (cBAT) and subcutaneous white adipose tissue (sWAT) of Myf5-BMPR1A-KO mice and control littermates, and differentiated as described before[10].

Immortalized pre-adipocytes

Immortalized cell lines were generated as earlier described[37]. In brief, cBAT from individual newborn pups (postnatal day 1 or 2) of homozygous floxed parents for the respective BMP-receptor was collected and pre-adipocytes were isolated by enzymatic digestion. Pre-adipocytes were immortalized by infection with SV40-expressing lentivirus and subsequent selection with puromycin. Stable cell lines were then infected with adenovirus expressing either GFP (control) or a CRE::GFP fusion construct for *in vitro* recombination (Gene Transfer Vector Core, University of Iowa, Iowa City, IA). 48 h post-infection, GFP^{pos} cells were collected by flow cytometry and expanded for subsequent use in experiments. DNA was isolated for PCR-analysis to determine full recombination of the respective receptor gene using the primers as detailed above.

Cell culture

Pre-adipocyte cell lines were cultured as described before[11], except that 2% fetal bovine serum was used during differentiation. BMP7-treatments (3.3 nM) were performed for three days prior to 48 h of adipogenic induction, followed by a differentiation period of 5 days. Oil Red O staining was performed as described before[11].

Thermal imaging of skin surface temperature

Measurement of skin temperature was performed using a thermal imaging camera (T300 InfraRed Camera; FLIR Systems, Inc., North Billerica, MA). Skin surface temperature of newborns was analyzed using FLIR Reporter 8.5 software (FLIR Systems, Inc.). Images were acquired by placing newborn mice of the same litter (P4-P6) in 6-well cell culture dishes, and 2-3 images of each mouse from different angles were acquired in order to minimize temperature variations due to different postures of the animal. Software drawing tools were used to draw a region of interest (ROI) around the entire animal, and average body surface temperature was calculated using that ROI. For each animal, an average temperature value of the temperatures from all single images was calculated. These averages were then used for statistical analysis.

Serum parameters

Serum levels of norepinephrine (NE) were determined using a commercially available ELISA-kit and according to the manufacturer's instructions (Norepinephrine (Research) ELISA; IBL-America, Minneapolis, MN). To stabilize norepinephrine, 1 mM EDTA and 4 mM sodium metabisulfite were added to the serum. Serum was prepared by spinning freshly collected blood in a cooled centrifuge at 6.000 g for 20 min. The clear supernatant was

collected and stored at −80°C. Samples were analyzed within 12 weeks after collection. To determine circulating irisin levels, a commercially available ELISA assay kit was used according to the manufacturer's specifications (Phoenix Pharmaceuticals, Inc., Burlingame, CA).

Body composition

Relative contents of lean and fat mass were determined using Dual-energy X-ray absorptiometry (DEXA) according to the manufacturer's instructions (GE Lunar PIXImus 2, General Electric Medical Systems, Pewaukee, WI). Animals were anaesthetized with pentobarbital (50 mg/kg, i.p.) and placed in the scanning area to measure body composition. Relative lean and fat mass were calculated by normalizing to body weight.

Norepinephrine-induced thermogenic capacity

Measurement of maximum thermogenic capacity was performed as described before with some modifications[12,28]. Animals were maintained in the cold as described above for 8 days before the experiment. All measurements were performed at room temperature. Oxygen consumption (OC) by indirect calorimetry was assessed using the Comprehensive Lab Animal Monitoring System (CLAMS, Columbus Instruments, Columbus, OH) and the Oxymax for Windows software (version 4.58) for data analysis. Animals were anaesthetized with pentobarbital (80 mg/kg, i.p.), and indirect calorimetry was performed immediately for 30 min to record basal values of OC. The sampling interval was set to 15 min to allow for stable OC assessment throughout the experiment. After three data points were obtained, animals were briefly removed from the chamber and NE was injected subcutaneously (1 mg norepinephrine bitartrate/kg, Sigma-Aldrich), and OC was recorded for another 90 minutes. To determine maximum NE-induced thermogenic capacity (VO2), the average value for basal OC prior to NE-injection was calculated and subtracted from the average value of highest NE-induced OC (t_{60} and t_{75}). Areas under the curve (AUC) were calculated for the curves after NE-injection. Data were presented either not normalized, i.e. per animal, or after normalization to total body weight, or total fat mass (from DEXA scan).

Denervation of cBAT

Denervation of cBAT was performed as described before[38]. C57BL/6J mice (The Jackson Laboratory) aged 6 weeks were used for denervations. In brief, mice were anaesthetized and placed on a warm pad to maintain body temperature. Under a stereomicroscope, an incision was made posterior to the interscapular cBAT pad. Surrounding muscle and white fat was carefully moved to the side and the cBAT pad was turned upward to expose the five branches of the intercostal nerve bundles. Denervation was performed by isolating and cutting the nerve bundles and removing a portion of about 1-2 mm from each strand. Care was taken not to damage the adjacent blood vessels. The procedure was performed on left and right lobes of the interscapular brown fat. BAT pads, surrounding white fat, and muscle were placed in the original locations and the incision was closed using tissue adhesive glue (Vetbond, 3M Animal Care Products, St. Paul, MN). The same procedure was performed for sham surgeries, except that nerve bundles were not cut. Animals were housed in single cages and monitored daily during the first week of recovery. After 10 weeks, animals were divided in four groups of (1) sham-operated mice receiving vehicle i.p.-injections (PBS), (2) sham-

operated mice receiving injections of CL316,243 as described above, (3) denervated mice receiving vehicle or (4) Cl316,243.

Statistical analysis

All statistical analyses were performed using the programs Excel (Microsoft Corporation, Redmond, WA), Statview (SAS Institute Inc., Cary, NC) and GraphPad Prism (GraphPad Software, Inc, CA). Statistical analyses were performed using two-tailed Student's t-test or ANOVA for comparing the means of two or multiple groups, respectively. Nonparametric testing (U-Mann-Whitney test) was used where appropriate, i.e. when normal distribution of sample sets was not evident. The means of two groups were considered significantly different when the p-value was smaller than 0.05.

Supplementary Material

Refer to Web version on PubMed Central for supplementary material.

Acknowledgments

Reference List

1. Cannon B, Nedergaard J. Metabolic consequences of the presence or absence of the thermogenic capacity of brown adipose tissue in mice (and probably in humans). Int J Obes Lond. 2010; 34(1):S7–16. [PubMed: 20935668]

2. Cypess AM, et al. Identification and importance of brown adipose tissue in adult humans. N Engl J Med. 2009; 360:1509–1517. [PubMed: 19357406]

3. Nedergaard J, Bengtsson T, Cannon B. Unexpected evidence for active brown adipose tissue in adult humans. Am J Physiol Endocrinol Metab. 2007; 293:E444–452. [PubMed: 17473055]

4. van Marken Lichtenbelt WD, et al. Cold-activated brown adipose tissue in healthy men. N Engl J Med. 2009; 360:1500–1508. [PubMed: 19357405]

5. Virtanen KA, et al. Functional brown adipose tissue in healthy adults. N Engl J Med. 2009; 360:1518–1525. [PubMed: 19357407]

6. Guerra C, Koza RA, Yamashita H, Walsh K, Kozak LP. Emergence of brown adipocytes in white fat in mice is under genetic control. Effects on body weight and adiposity. J Clin Invest. 1998; 102:412–420. [PubMed: 9664083]

7. Almind K, Manieri M, Sivitz WI, Cinti S, Kahn CR. Ectopic brown adipose tissue in muscle provides a mechanism for differences in risk of metabolic syndrome in mice. Proc Natl Acad Sci USA. 2007; 104:2366–2371. [PubMed: 17283342]

8. Wu J, et al. Beige adipocytes are a distinct type of thermogenic fat cell in mouse and human. Cell. 2012; 150:366–376. [PubMed: 22796012]

9. Petrovic N, et al. Chronic peroxisome proliferator-activated receptor gamma (PPARgamma) activation of epididymally derived white adipocyte cultures reveals a population of thermogenically competent, UCP1-containing adipocytes molecularly distinct from classic brown adipocytes. J Biol Chem. 2010; 285:7153–7164. [PubMed: 20028987]

10. Schulz TJ, et al. Identification of inducible brown adipocyte progenitors residing in skeletal muscle and white fat. Proc Natl Acad Sci USA. 2011; 108:143–148. [PubMed: 21173238]

11. Tseng YH, et al. New role of bone morphogenetic protein 7 in brown adipogenesis and energy expenditure. Nature. 2008; 454:1000–1004. [PubMed: 18719589]

12. Whittle AJ, et al. BMP8B increases brown adipose tissue thermogenesis through both central and peripheral actions. Cell. 2012; 149:871–885. [PubMed: 22579288]

13. Seale P, et al. PRDM16 controls a brown fat/skeletal muscle switch. Nature. 2008; 454:961–967. [PubMed: 18719582]

14. Timmons JA, et al. Myogenic gene expression signature establishes that brown and white adipocytes originate from distinct cell lineages. Proc Natl Acad Sci USA. 2007; 104:4401–4406. [PubMed: 17360536]

15. Atit R, et al. Beta-catenin activation is necessary and sufficient to specify the dorsal dermal fate in the mouse. Dev Biol. 2006; 296:164–176. [PubMed: 16730693]

16. Lepper C, Fan CM. Inducible lineage tracing of Pax7-descendant cells reveals embryonic origin of adult satellite cells. Genesis. 2010; 48:424–436. [PubMed: 20641127]

17. Schmid P, Lorenz A, Hameister H, Montenarh M. Expression of p53 during mouse embryogenesis. Development. 1991; 113:857–865. [PubMed: 1821855]

18. Sanchez-Gurmaches J, et al. PTEN loss in the Myf5 lineage redistributes body fat and reveals subsets of white adipocytes that arise from Myf5 precursors. Cell Metab. 2012; 16:348–362. [PubMed: 22940198]

19. Buckingham ME, Lyons GE, Ott MO, Sassoon DA. Myogenesis in the mouse. Ciba Found Symp. 1992; 165:111–131. [PubMed: 1516464]

20. Kishigami S, Mishina Y. BMP signaling and early embryonic patterning. Cytokine Growth Factor Rev. 2005; 16:265–278. [PubMed: 15871922]

21. Gupta RK, et al. Transcriptional control of preadipocyte determination by Zfp423. Nature. 2010; 464:619–623. [PubMed: 20200519]

22. Farmer SR. Transcriptional control of adipocyte formation. Cell Metab. 2006; 4:263–273. [PubMed: 17011499]

23. Cannon B, Nedergaard J. Nonshivering thermogenesis and its adequate measurement in metabolic studies. J Exp Biol. 2011; 214:242–253. [PubMed: 21177944]

24. Fisher FM, et al. FGF21 regulates PGC-1alpha and browning of white adipose tissues in adaptive thermogenesis. Genes Dev. 2012; 26:271–281. [PubMed: 22302939]

25. Bostrom P, et al. A PGC1-alpha-dependent myokine that drives brown-fat-like development of white fat and thermogenesis. Nature. 2012; 481:463–468. [PubMed: 22237023]

26. Collins S. beta-Adrenoceptor Signaling Networks in Adipocytes for Recruiting Stored Fat and Energy Expenditure. Front Endocrinol (Lausanne). 2011; 2:102. [PubMed: 22654837]

27. Tseng YH, Cypess AM, Kahn CR. Cellular bioenergetics as a target for obesity therapy. Nat Rev Drug Discov. 2010; 9:465–482. [PubMed: 20514071]

28. Feldmann HM, Golozoubova V, Cannon B, Nedergaard J. UCP1 ablation induces obesity and abolishes diet-induced thermogenesis in mice exempt from thermal stress by living at thermoneutrality. Cell Metab. 2009; 9:203–209. [PubMed: 19187776]

29. Rothwell NJ, Stock MJ. Surgical removal of brown fat results in rapid and complete compensation by other depots. Am J Physiol. 1989; 257:R253–258. [PubMed: 2548406]

30. Xue B, et al. Genetic variability affects the development of brown adipocytes in white fat but not in interscapular brown fat. J Lipid Res. 2007; 48:41–51. [PubMed: 17041251]

31. Dudas M, Sridurongrit S, Nagy A, Okazaki K, Kaartinen V. Craniofacial defects in mice lacking BMP type I receptor Alk2 in neural crest cells. Mech Dev. 2004; 121:173–182. [PubMed: 15037318]

32. Mishina Y, Hanks MC, Miura S, Tallquist MD, Behringer RR. Generation of Bmpr/Alk3 conditional knockout mice. Genesis. 2002; 32:69–72. [PubMed: 11857780]

33. Tallquist MD, Weismann KE, Hellstrom M, Soriano P. Early myotome specification regulates PDGFA expression and axial skeleton development. Development. 2000; 127:5059–5070. [PubMed: 11060232]

34. Abel ED, et al. Adipose-selective targeting of the GLUT4 gene impairs insulin action in muscle and liver. Nature. 2001; 409:729–733. [PubMed: 11217863]

35. Yi SE, Daluiski A, Pederson R, Rosen V, Lyons KM. The type I BMP receptor BMPRIB is required for chondrogenesis in the mouse limb. Development. 2000; 127:621–630. [PubMed: 10631182]

36. Kaufman, MH. The Atlas of Mouse Development. Vol. 1. Academic Press Limited; 1992.

37. Klein J, Fasshauer M, Klein HH, Benito M, Kahn CR. Novel adipocyte lines from brown fat: a model system for the study of differentiation, energy metabolism, and insulin action. Bioessays. 2002; 24:382–388. [PubMed: 11948624]

38. Pulinilkunnil T, et al. Adrenergic regulation of AMP-activated protein kinase in brown adipose tissue in vivo. J Biol Chem. 2011; 286:8798–8809. [PubMed: 21209093]
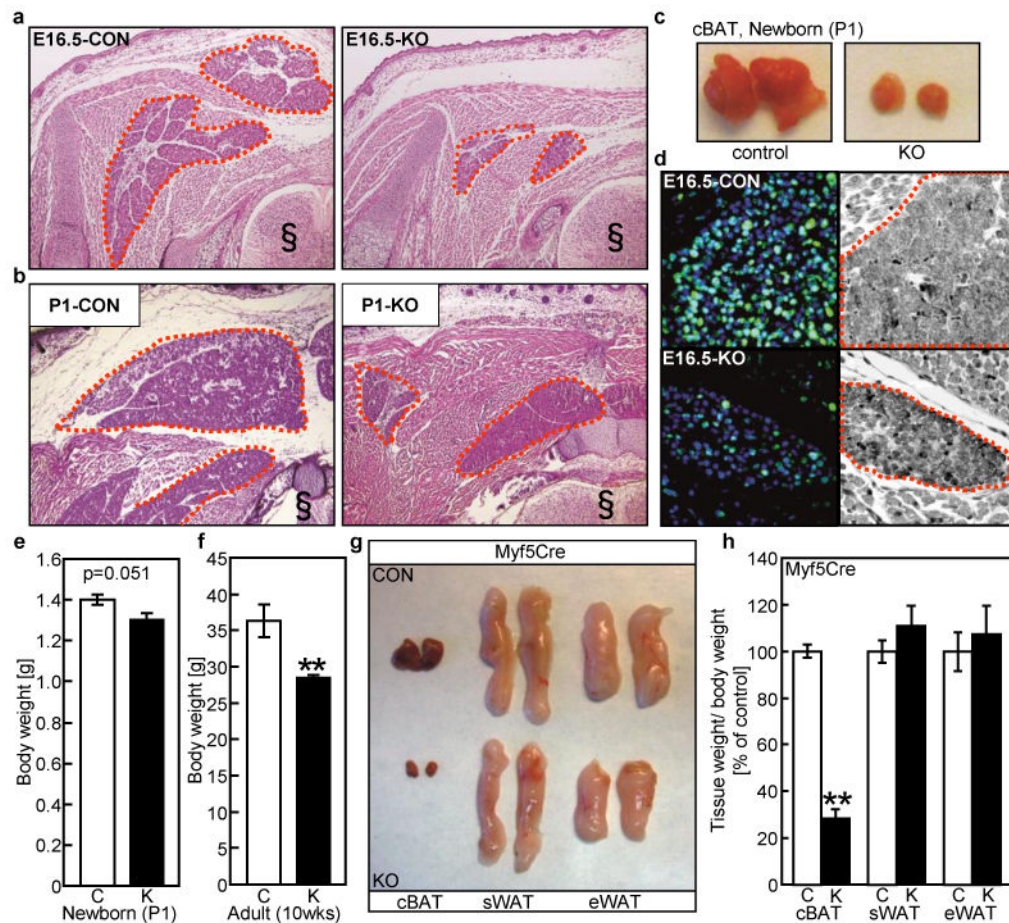
Figure 1. Loss of *Bmpr1A* impairs cBAT-formation by decreasing embryonic progenitor proliferation

a, **b**, H&E-staining of interscapular sections at embryonic stage E16.5 and in newborns (P1). Photographs (100× original magnification) of the same anatomical location of transversal sections were acquired for control (CON) and Myf5-BMPR1A-KO mice (KO; **§** indicates spinal cord, orange lines indicate brown fat; applies to all panels). **c**, Macroscopic images of cBAT of P1-newborns. **d**, Ki67-immunofluorescence (green) of cBAT at E16.5 and co-localization with nuclear DAPI-stain (blue, left panels; Analysis of Ki67^{pos} nuclei in Supplementary Figure 1d), and light microscopy of the same area (right panels, 400× original magnification). **e**, **f**, Body weight analysis of control (C) and Myf5-BMPR1A-KO (K) mice from P1-newborns (e; n=12/4) and adult mice (f; n=6). **g**, **h**, Analysis of cBAT-, sWAT-, and eWAT-weights after normalization to body weight (n=13). All data are presented as mean ± s.e.m. Asterisks denote significant differences between genotypes: ** P < 0.01.
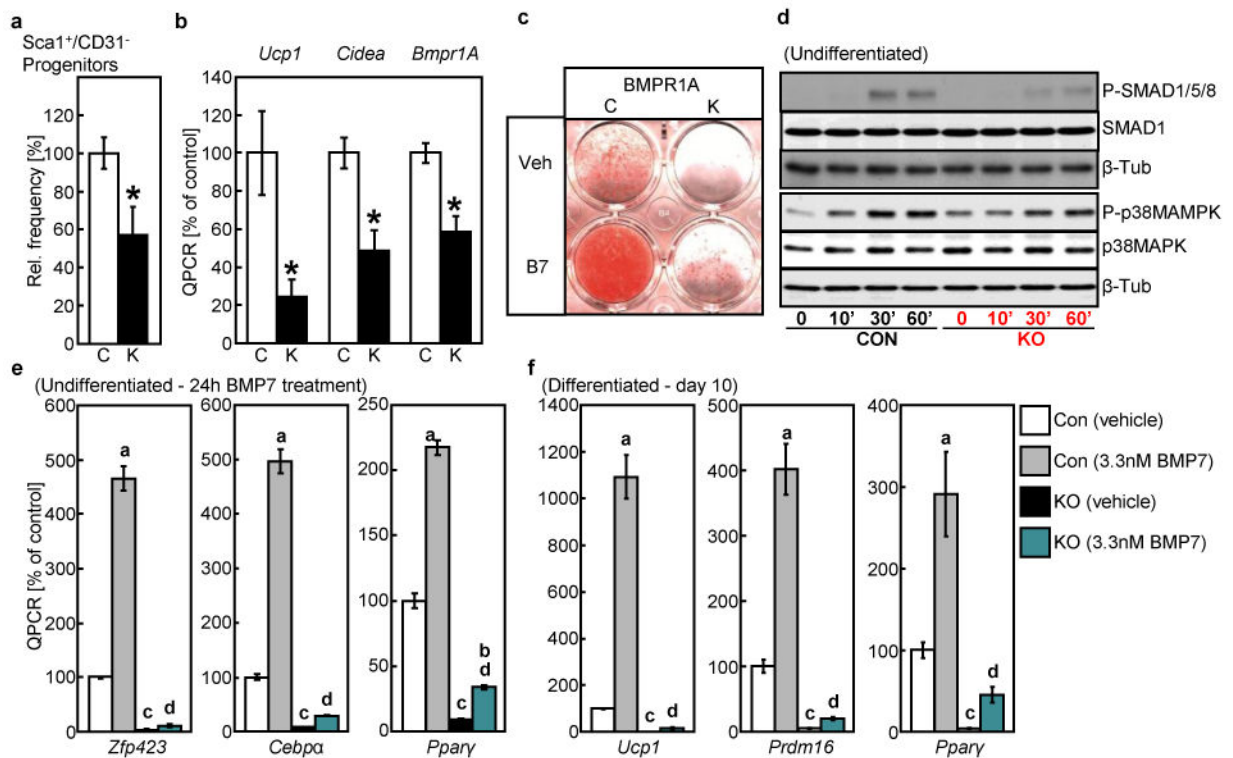
**Figure 2. Ablation of *Bmpr1A* in brown pre-adipocytes derived from the Myf5^{pos} lineage inhibits differentiation**

a, Relative frequency of Sca1^{pos}/CD31^{neg}/CD11b^{neg}/CD45^{neg} adipogenic progenitors of the Myf5-CRE(YFP)[pos] lineage in cBAT after normalization to tissue weight (n=6). White bars indicate cells isolated from control mice (C), black bars indicate Myf5-BMPR1A-KO cells (K). **b**, qPCR analysis of *Ucp1*, Cell death-inducing DFFA-like effector a (*Cidea*), and *Bmpr1A* mRNAs in FACS-purified primary progenitors from cBAT after adipogenic differentiation (n=3). Asterisks denote significant differences between genotypes: * $P <$ 0.05. **c**, Triglyceride-specific Oil Red O staining of differentiated control (C) or BMPR1A-deficient (K) immortalized pre-adipocyte cell lines pretreated with vehicle (Veh) or BMP7 (B7). **d**, Western blot of phospho-Smad1/5/8 (1st row), basal Smad1 (2nd row), corresponding α-Tubulin (3rd row), phospho-p38MAPK (4th row), basal p38MAPK (5th row), and corresponding α-Tubulin (6th row) in undifferentiated control (CON) and pre-adipocytes lacking BMPR1A (KO) following exposure to BMP7 for 10, 30, and 60 minutes. Representative blots from three independent experiments are shown. **e**, qPCR of zinc-finger protein 423 (*Zfp423*), CCAAT/enhancer-binding protein-alpha (*Cebpα*), and peroxisome proliferator-activated receptor-gamma (*Pparγ*) in undifferentiated brown pre-adipocytes after 24h-exposure to BMP7. **f**, qPCR of *Ucp1*, PR-domain-containing-16 (*Prdm16*), and *Pparγ* isolated from mature brown adipocytes. Pre-adipocytes were treated with BMP7 for 3 days, followed by 7-day differentiation. All experiments were performed in triplicate and are presented as mean ± s.e.m. For panels e and f, statistically significant differences as determined by ANOVA ($p < 0.05$) were [a]control (vehicle) vs. control (BMP7); [b]KO (veh) vs. KO (BMP7); [c]control (veh) vs. KO (veh); and [d]control (BMP7) vs. KO (BMP7).
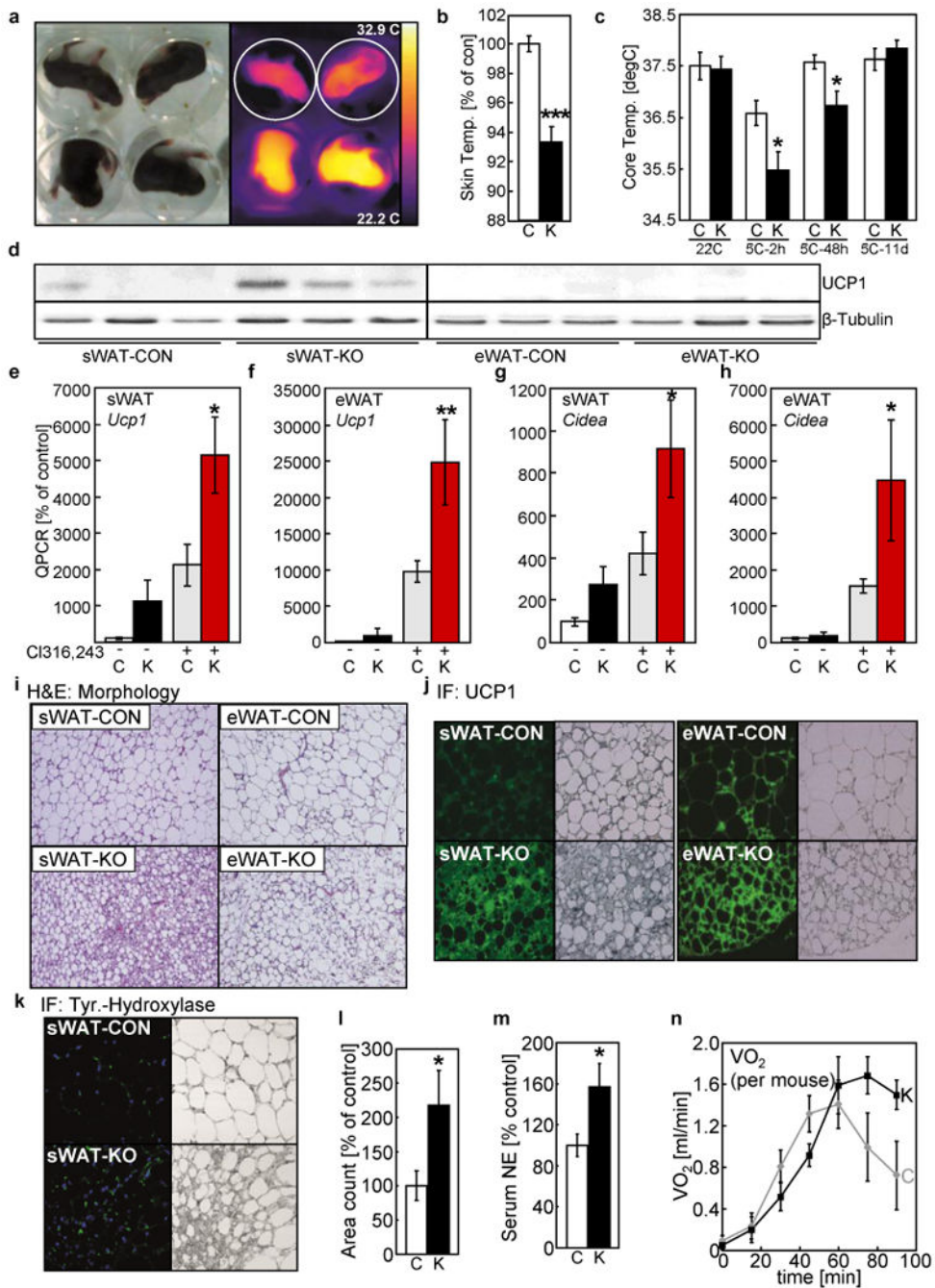
Figure 3. Specific ablation of cBAT results in a compensatory response of increased browning by enhanced sympathetic input to WAT

a, Photographic (left side) and infrared (right side) images of P4-P6 newborns, indicating KO pups by white circles. **b**, Quantification of average skin surface temperature from infrared images. White bars indicate control mice (C), black bars Myf5-BMPR1A-KOs (K; n=12/10). **c**, Body core temperature of adult control and Myf5-BMPR1A-KO mice. Measurements were performed at room temperature (22°C, n=11/10), and following 2 h (n=5), 48 h (n=7/6), and 11 days (n=7/6) of cold exposure (5°C). **d**, Western blot analysis of

UCP1 in sWAT and eWAT. **e**, **f**, qPCR of *Ucp1* gene expression in sWAT (e) and eWAT (f). Grey bars indicate controls after administration of β3-adrenergic agonist CL316,243 (1 mg/kg body weight) for ten days, red bars indicate CL316,243-injected Myf5-BMPR1A-KO (n=7; applies to all panels). **g**, **h**, qPCR of *Cidea* in sWAT (g) and eWAT (h). **i**, H&E staining of sWAT and eWAT after administration of CL316,243 (original magnification: 200×). **j**, UCP1-immunofluorescence (IF) of sWAT and eWAT after administration of CL316,243 (original magnification: 400×). Left panels show UCP1-IF (green), right panels show light microscopic image of the same area. **k**, **l**, Tyrosine hydroxylase-IF and quantification of TH[pos] nerve fibers in sWAT after administration of CL316,243 (original magnification: 400×). (n=3). **m**, Serum levels of norepinephrine (n=8). n, Time course of NE-induced oxygen consumption in mice maintained at 5°C for 8 days (control - gray line; KO - black line; n=5). All data are presented as mean ± s.e.m. Asterisks denote significant differences between genotypes: * $P < 0.05$; ** $P < 0.01$.
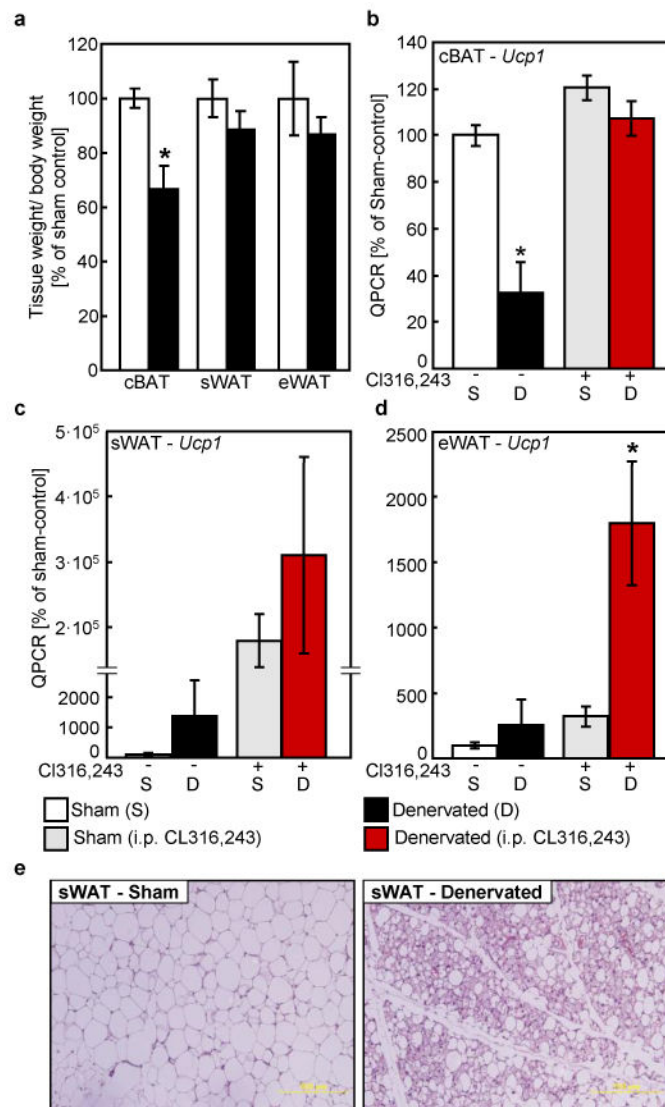
Figure 4. Loss of sympathetic innervation causes atrophy of cBAT and compensatory browning of white fat

a, Tissue weight of cBAT, sWAT, and eWAT normalized to body weight in sham-operated mice (S, white bars) and mice after surgical denervation of cBAT (D, black bars). **b, c, d,** qPCR of *Ucp1* in cBAT (b), sWAT (c), and eWAT (d) of control mice, denervated mice, controls (S, grey bars) or denervated (D, red bars) mice injected with CL316,243. **e**, H&E staining of sWAT from sham-operated and cBAT-denervated mice after CL316,243-injections. All data are presented as mean ± s.e.m (n=4). Asterisks denote significant differences between denervation and respective control groups: * P < 0.05 as determined by ANOVA.